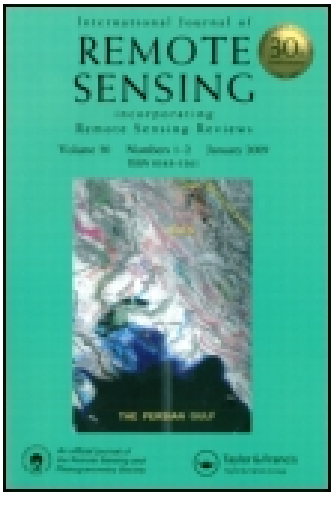

International Journal of Remote Sensing

Publication details, including instructions for authors and subscription information:
http://www.tandfonline.com/loi/tres20

Predicting salinity in tomato using soil reflectance spectra

N. Goldshleger [a] , A. Chudnovsky [b] & R. Ben-Binyamin [a]

[a] Soil Erosion Research Station, Soil Conservation and Drainage Division, Ministry of Agriculture , Israel

[b] Harvard School of Public Health, Department of Environmental Health, Harvard University , Boston , MA , USA

Published online: 02 May 2013.

To cite this article: N. Goldshleger , A. Chudnovsky & R. Ben-Binyamin (2013) Predicting salinity in tomato using soil reflectance spectra, International Journal of Remote Sensing, 34:17, 6079-6093, DOI: 10.1080/01431161.2013.793859

To link to this article: http://dx.doi.org/10.1080/01431161.2013.793859

International Journal of Remote Sensing, 2013
Vol. 34, No. 17, 6079–6093, http://dx.doi.org/10.1080/01431161.2013.793859

Taylor & Francis
Taylor & Francis Group

Predicting salinity in tomato using soil reflectance spectra

N. Goldshleger[a]*, A. Chudnovsky[b], and R. Ben-Binyamin[a]

[a]*Soil Erosion Research Station, Soil Conservation and Drainage Division, Ministry of Agriculture, Israel;* [b]*Harvard School of Public Health, Department of Environmental Health, Harvard University, Boston, MA, USA*

(*Received 26 May 2011; accepted 21 January 2013*)

Soil salinity is one of the most common soil degradation processes, found particularly in both arid and semi-arid areas. Salt (Cl)- and sodium (Na)-affected soils impact vegetation and plant communities. Under these conditions, soil salinity can serve as an indicator of vegetation salinity. In this study, we explored whether spectroscopy could quantitatively assess foliar Cl and Na concentration as indicators to assess salinity in tomato plants. Reflectance spectra of soil samples were obtained in the 400–2500 nm region using a hyperspectral radiometer. The relationship between the Na and Cl contents of tomato plants growing in various saline environments and soil spectral reflectance was determined using partial least squares regression. The Cl-content model was more accurate for determining leaf salinity ($R^2 = 0.92$, root mean square error of prediction (RMSEP) = 0.2%) than the Na-content model ($R^2 = 0.87$, RMSEP = 0.6%). We conclude that reflectance spectroscopy is potentially useful for characterizing the key properties of salinity in growing vegetation and assessing its salt quality. The results of this study can serve as a starting point in precision agriculture for salinity measurements in tomato fields and could be further upgraded for use by airborne/satellite remote-sensing modes.

1. Introduction

Saline- or salt-affected soils are prevalent in both arid and semi-arid regions, with high levels of evapotranspiration and irrigated agriculture (Gleick 1993). The degradation of soils in the Jezreel Valley, one of Israel's most important agricultural areas, is a good example of this phenomenon. Over the years, this area has experienced large increases in soil salinity resulting from the use of saline water (Metternicht 1998). This practice can lead to crop damage if salinity levels exceed plant tolerance limits. Therefore, crop monitoring is critical for taking timely corrective action, such as drainage system construction (Zinck and Metternicht 2009).

Conventional methods of monitoring changes in soil salinity are based on field observation and laboratory analyses of both crops and soils. This is mostly done by measuring the electrical conductivity (EC) of the soil solution as well as the exchangeable sodium percentage (ESP) and pH. However, these methods are time-consuming, expensive, and restricted to certain areas.

Reflectance spectroscopy is one of the fastest-growing analytical technologies globally, with an overwhelming application in virtually all the fields of science (e.g. Williams and

*Corresponding author. Email: Goldshleger@gmail.com

Norris 1987; Demattê et al. 2004). In general, all compounds exhibit absorption/emission spectra that can be analysed both quantitatively and qualitatively. Specifically, visible–near infrared–shortwave infrared spectra (VIS–NIR–SWIR: 400–2500 nm) provide key aspects of both organic and inorganic matter which constitute invaluable diagnostic information for environmental scientists. Salt mineralogy (e.g. carbonates, sulphates, chlorides) determines the presence (or absence) of absorption bands in the electromagnetic spectrum. For instance, pure halite (NaCl) is transparent and its chemical composition and structure preclude absorption in the visible and near to thermal IR bands (Hunt, Salisbury, and Lenhoff 1972). Middle-IR bands, reflecting water and OH absorption, allow differentiation between chlorides (as halite) and sulphates when both are dry. Mulders (1987) reported the 1500–1730 nm range as one of the absorption regions for soil-surface features containing gypsum ($CaSO_4 \cdot H_2O$). By inhibiting growth, soil salinity influences the spectral reflectance of vegetation features (Rud, Shoshany, and Alchanatis 2011). Therefore, crop canopy reflectance is indirectly related to soil salinity (Zhang et al. 1997; Szabo et al. 1998). Importantly, salt has no spectral fingerprints across the VIS-NIR-SWIR spectral range. To the best of our knowledge, there is no study by reflectance spectroscopy on the interaction between soil and vegetation salinity.

In this study, we propose employing soil reflectance spectroscopy to predict the Na or Cl content of tomato growing in various saline environments. We selected tomato because it is one of the main field crops grown in the Jezreel region, where saline water is used for its irrigation (Cuartero et al. 2006). Multivariate data analysis based on partial least squares (PLS) regression was carried out to assess plant salinity from soil reflectance data. We used Cl and Na contents measured in tomato plants as tracers for soil salinity.

2. Materials and methods

2.1. The study area

We selected two irrigated fields in the Jezreel Valley (northern Israel) that are affected seasonally by soil salinity: Ifat and Mizra (Figure 1).

High hydrodynamic pressure is created in the upper soil layer by a buried riverbed with restricted exit, inhibiting the lowering of groundwater levels by means of subsurface drainage systems. The resultant shallow saline water table contributes significantly to increased salinity in the root zone (Mirlas et al. 2003). The Ifat field, extending over some 50 ha, is bounded on the south by the embankment of the large Genigar Reservoir. As a result of this reservoir's impact on the upper groundwater, groundwater levels rise close to the soil surface around the reservoir's embankment. Evaporation from this shallow groundwater contributes to the formation of saline soils. The soils of both fields are Chromic Vertisols, characterized by high smectite clay mineral content (Goldshleger et al. 2004). During the dry summer, wide and deep soil cracks increase deep percolation of irrigation water by preferential flow. During the winter rains or under summer irrigation, the soils swell and the cracks close, resulting in a considerable reduction in saturated hydraulic conductivity (Dan et al. 1976).

There is a salinity gradient to the north and Ifat field to the south by the embankment of the large Maale Kishon Reservoir. As a result of the supporting impact of the reservoir on the upper groundwater, the groundwater levels were elevated near to the soil surface around the embankment of the reservoir. Evaporation from these shallow groundwaters contributed to the formation of saline soils.

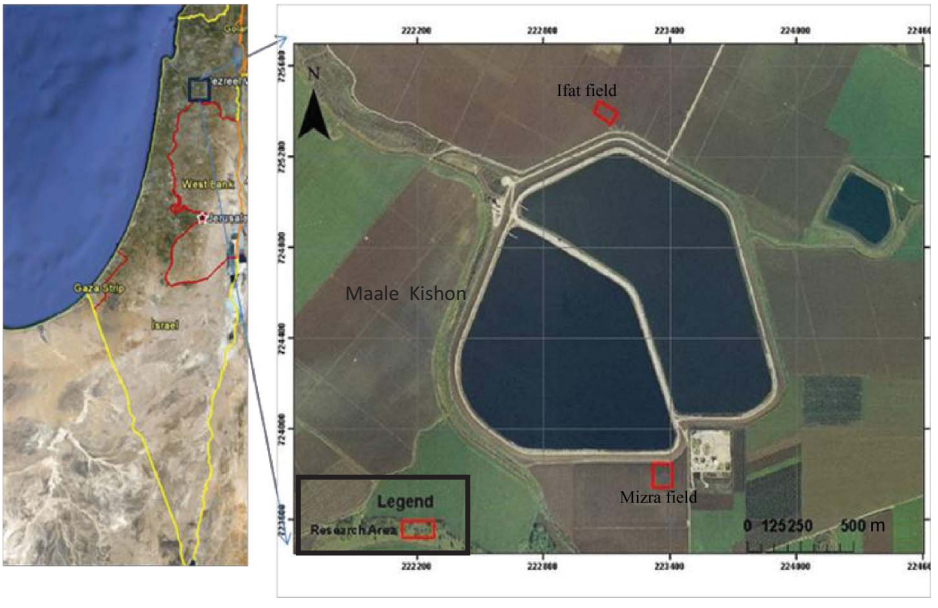

Figure 1. Location of Jezreel Valley on a map of Israel (left), with the two study fields bordering the Genigar Reservoir (right).

Figure 2. Tomato planted in rows in the irrigated field at Mizra, marking the sampling locations for soils and plants.

2.2. Sample description

2.2.1. Soil sampling

In each field, soil samples were obtained at points located at 20 m intervals along three 100 m transects aligned to capture the salinity gradient (Figure 2). Furthermore, subsamples were taken at each point at depth increments of 0–30 cm using an auger (diameter 5 cm)

and then bulked into one sample per point. These samples were then placed into plastic bags for laboratory analysis. A total of 72 soil samples were collected from the two fields.

2.2.2. Tomato sampling

Tomato leaves were sampled along the transects within a 0.2 m radius of the soil sampling points, with each sample including 3 leaves. Twenty-two leaf samples were taken from the Mizra field and 50 from Ifat, giving a total of 72 tomato plant samples. The plants were fertilized prior to the growth stage at which they produce fruit, and were in the reproduction stage during spectral measurements. The plants and the soil were sampled simultaneously.

2.3. Chemical analyses

The soil samples were dried at 65–70°C for 72 hours and milled to a size of 2 mm (by passage through a 10 mesh sieve). For soil samples, sodium (Na) and chloride (Cl) contents (both mg/l) in the soil solution extracted from saturated paste were analysed by flame photometry and calometry (titration with $AgNO_3$ solution), respectively. For plant samples, Na content (%W) was analysed by flame photometry following digestion with H_2SO_4 and H_2O_2. Cl content (%W) was analysed by chloridimetry following extraction with 0.1 N HNO_3 (Hille 1998; Kalra 1998).

2.4. Spectral reflectance measurements

Immediately following chemical analyses, spectral reflectance measurements were obtained in the laboratory by scanning oven-dried soil samples with an Analytical Spectral Devices (ASD; Boulder, CO, USA) Full-Range (FR) spectrometer (Figure 3). The FR spectrometer samples a spectral range of 350–2500 nm, and uses three detectors spanning the VIS and NIR (VNIR, comprising a Si photodiode array) and shortwave infrared (SWIR1 and SWIR2, comprising two separate InGaAs photodiodes). Spectral resolution, as defined by full width half max, is 3 nm in the VNIR region and 10 nm in the SWIR region.

All soil samples were held in a glass dish with a black carbon background placed underneath (Figure 3). Spectral reflectance was measured in the laboratory by attaching the high-intensity contact probe (‘potato’) to the soil sample. The ‘potato’, which uses a tungsten halogen lamp for artificial illumination, was set on a stable tripod base and maintained in a constant position at a nadir-angle. The fibre optical cable from the ASD spectrometer is joined to the stable tripod, which has a handle allowing vertical movement of the ‘potato’ relative to the soil sample. For each soil sample, three spectral measurements were taken and averaged (each reflectance measurement includes an average of 40 readings).

For all experiments, $BaSO_4$ powder of the same geometry as each soil sample was used as a white reference to enable conversion of the radiance data to reflectance values.

2.5. Data analyses

Cl and Na contents, which are indicators of the presence of salinity in soil and vegetation, were selected as the soil properties to be investigated in relation to spectroscopy. First, we analysed the changes in Na and Cl contents occurring at 0–30 cm soil depth and compared these with changes in Na and Cl contents occurring in the tomato plants. Next, we correlated the soil contents of Na and Cl with the chemical properties of the corresponding leaves.

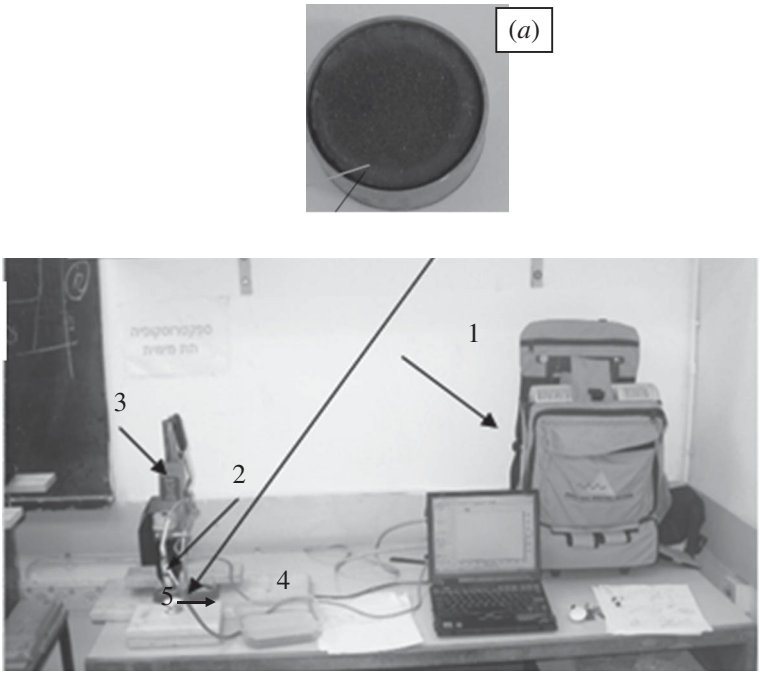

Figure 3. Field spectroradiometer (1) with glass dish placed above a black carbon background (*a*); high-intensity contact probe 'potato' (2), stable tripod base (3), and fibre optic cable from spectrometer (4).

2.6. Multivariate calibration analyses

Multivariate calibration models were generated using PLS regression (Esbensen 2002), with the goal being to define a relationship between the VIS–NIR–SWIR spectra (400–2400 nm) of soil samples and leaf contents of Na or Cl as an indicator of salinity in tomato leaves:

$$Y = A + A_1X_1 + A_1X_1 + A_1X_1 + \cdots + A_nX_n, \quad (1)$$

where Y is the chemically measured Na *versus* Cl contents of a leaf sample, A is an empirical coefficient, and X is the soil spectral reflectance at a specific wavelength. The PLS regression is based on latent variable decomposition of two blocks of a variable's X matrix based on soil spectral data and Y matrix based on measured vegetation salinity data.

Since there were a limited number of samples, statistical parameters for the calibration model were calculated by leave-one-out cross-validation (only one sample at a time is omitted from the calibration and used for prediction). Leave-one-out cross-validation is the best alternative when there are insufficient samples for a separate test set (Esbensen 2002). To confirm the quality of the model, besides internal validation, we used another independent validation set: from the total of 72 samples, a cross-calibration set consisted of 57 samples and the remaining 15 samples were used as a test set for prediction. The quality of the model was assessed using this group of separated samples to form the test set rather than the samples used to optimize the model. Since the basic requirement for the test set is to be as similar as possible to the calibration set, with regard to both population

and sampling conditions, we used PCA analyses (PCA transforms the original independent variables (wavelengths) into new axes, or principal components (PCs). These PCs are orthogonal, so that the data sets presented on these axes are uncorrelated with each other (Esbensen 2002). The spectral patterns derived using PCA provide information about the characteristic peaks, indicating which are the most significant ones when discriminating soil samples) to identify spectrally similar samples and those having similar Na and/or Cl contents to those of the calibration set. These samples were then manually separated and used as a separate test set. This is required to ensure that the populations selected provide stable chemical and spectral assessments, which can form the basis for reliable prediction of soil properties.

The difference between the predicted and measured Cl and Na contents (measured separately) was expressed as RMSEP. RMSEP is the direct estimate of the prediction and modelling errors, expressed in original units, and is defined as the square root of the average of the squared differences between the predicted and measured values of the validation objects (Esbensen 2002):

$$\mathrm{RMSEP} = \left[\frac{\sum \left(X_{\mathrm{m}} - X_{\mathrm{p}}\right)^2}{n_{\mathrm{v}}}\right]^{1/2}, \tag{2}$$

where X_{m} is the chemically measured salinity of the sample, X_{p} is the predicted value of the sample on the basis of spectral analysis, and n_{v} is the number of samples in the calibration stage. Root mean square error of cross-validation (RMSECV) is a measure of a model's ability to predict new samples. RMSECV is defined as the square root of the average of the squared differences between the predicted and measured values of the cross validation objects (Esbensen 2002). RMSECV is related to the PRESS value for the number of latent variables (LV components) included in the model:

$$\mathrm{RMSECV} = \sqrt{\frac{\mathrm{PRESS}}{n}}, \tag{3}$$

where PRESS is the sum of squares prediction error. PRESS is calculated via leave-one-out cross-validation (each sample is left out of the model and predicted once).

In addition, we used the ratio of prediction to deviation (RPD), which is defined as the ratio of standard deviation of the reference values (e.g. STDEV of infiltration rates) to the RMSECV or RMSEP (Mouazen et al. 2005):

$$\mathrm{RPD} = \frac{\mathrm{STDEV_{IR}}}{\mathrm{RMSECV\,(or\,RMSEP)}}, \tag{4}$$

for predicted *versus* measured salinity in cross-validation and prediction. R^2 indicates that the percentage of variance in the Y variable is accounted for by the X variable. An RPD value below 1.5 indicates that the model is unusable, between 1.5 and 2.0 indicates that the model has the potential to distinguish between high and low values, and between 2.0 and 2.5 indicates that quantitative prediction is possible. RPD values between 2.5 and 3.0 and above 3.0 indicate that the predictive capability of the model is excellent.

Initially, the spectral data considered were reflectance (R), absorbance ($-\log_{10}R$), and Kubelka–Munk units. To obtain a more linear relationship between spectral readings and the concentration of samples measured by reflectance, the spectra are usually converted to

absorbance or Kubelka–Munk units. To calculate Kubelka–Munk units, the reflectance (R) at each wavelength is calculated as follows (Mark 2000):

$$f(R) = (1 - R)^2 / 2R. \quad (5)$$

Next, the first derivative using the Savitzky–Golay algorithm was applied to each soil reflectance spectrum to remove extraneous spectral variation and create robust calibration models (Savitzky and Golay 1964; Mark 2000). The Savitzky–Golay method enables computation of first- or higher-order derivatives, including a smoothing factor that determines how many adjacent variables (wavelengths) will be used to estimate the polynomial approximation for the derivation.

We also investigated the influence of using the whole spectral region as well as individual selected wavelengths to generate an optimal PLS model to predict the Na or Cl content in tomato. Models were run on the entire wavelength region with the aim of identifying the significant wavelengths. Significant variables were estimated using Martens' uncertainty test (Esbensen 2002). Many plots and results are associated with the test, which allows estimation of the stability of a PLS regression model, identifying perturbing samples or variables, and selecting significant X variables. The test is performed with cross-validation over the whole spectral range. Therefore, each PLS model (raw and preprocessed) was first run on the whole range of spectra, and then restricted to significant wavelengths, which were identified based on Martens' test and previous knowledge of plant absorbencies. The model was then run solely on the selected wavelengths and reassessed until acceptable results (in terms of model stability and prediction accuracy) were achieved. All data management, calculations, PLS analyses, and different spectral pretreatments were performed using Unscrambler version 9.7 (Camo Software, Oslo, Norway).

3. Results

3.1. Chemical variations

For the purpose of definition, saline soils have an electrical conductivity of saturation extracts of more than 4 dS m^{-1} at 25°C. Soil salinity is measured as the salt concentration of the soil solution in terms of electric conductivity EC in dS m^{-1}. Sensitive plants are affected at half this salinity, and highly tolerant ones at about twice this level (Richards 1954). As can be seen from Table 1, on average, the soils studied were saline with an EC of 3.6. A high degree of variability in soil salinity is indicated by a standard deviation of 4.7, which exceeds the mean by more than 100%. Furthermore, although there was sufficient range in Na+ and Cl+ contents, the frequency distributions of Na+ and Cl+ concentration measurements were skewed to minimum values (Table 1). Consequently, we might expect that the predicted accuracy of Na+ and Cl+ in a final constructed model might be low. Also note that there is a relatively small dynamic range of salt content measured in tomato leaves (Table 1), which might also have an impact on model stability.

The relationships between soil and leaf Na content (Figure 4(a)) or soil and leaf Cl content (Figure 4(b)) have R^2 equal to 0.51 and 0.59, respectively. In other words, for Cl, approximately 59% of the variability in soil content can be explained by variability in Cl (%) leaf content. A similar comparison can be done for Na. Based on these linear regression results, we conclude that both Na and Cl contents measured in soil and leaves are related. The following section reports the results of calibrating the relationship between

Table 1. Average, standard deviation, median, minimum, and maximum values of Cl and Na concentrations in soil and tomato.

	Soil			Tomato leaves	
	Cl (mg kg^{-1})	Na (mg kg^{-1})	EC (dS m^{-1})	Cl (w%)	Na (w%)
Average	25.9	16.8	3.6	1.45	0.22
Standard deviation	37.05	14.73	4.7	0.63	0.07
Median	56	28	1.9	1.25	0.2
Minimum	2.7	3.4	0.6	0.75	0.12
Maximum	181.0	67.6	5.28	3.9	0.53

soil and leaf Na content, and soil and leaf Cl content, using multivariate data analysis, where wavelengths are additional explanatory variables based on PLS regression.

3.2. Calibration modelling

The importance of spectral salinity changes for the calibration is indicated from a plot of factor loadings (LVs or regression coefficients) *versus* wavelength (Figures 5 and 6). The dominant wavelengths identified by Martens' test for predicting Cl content were centred at: 400–540, 620, 700, 940, 990–1004, 1378, 1646, 1660, 1740, 1780, 2023, 2084, 2200–2240, 2350, and 2372 nm (Figure 5). The wavelengths selected for the prediction of Na content in soils were centred at 400–560, 720, 983, 1158, 1345, 1377, 1423, 1538, 1623, 1660, 1777, 1804, 1844, 1880, 1950, 2200–2240, and 2350 nm (Figure 6).

For the Cl calibration model, the first three loading vector (LV) components in the PLS model explained 95% of the X variance (spectra) and 90% of the Y variance (Cl). This indicates that most of the spectral variation is related to the Cl components modelled by PLS. For the Na calibration model, five LVs explained more than 98% of the X variance (spectra) and 88% of the Y variance (Na). For both models, the first three LVs alone accounted for 90% of the variance in the data, and the remainder of the loadings were responsible for only a small part of data variability.

The spectral range 500–700 nm represents the change in salinity levels and may be related to the presence of iron oxides (Clark 1999). The wavelengths centred at 950 and 2100 nm are associated with OH in water, clays (2200 nm), and calcite (2300 nm) (Hunt 1977; Clark 1999). The spectra at 1750, 1950, and 2200 nm are related to the presence of gypsum, which is a good indicator of the presence of halite (Ben-Dor et al. 2009).

Table 2 presents the results of PLS modelling of salinity using various models with raw and preprocessed spectra. The relatively high predictive ability of the external test set, at the validation test set level, enables us to surmise that our PLS models can be used to predict plant salinity based on soil spectral reflectance. As indicated by R^2 and RMSEP, PLS regression using first-derivative values and selected wavelengths to predict Cl content provided the best precision and accuracy of all models (Table 2), with a slope of near unity and Y intercept near zero (Figure 7). The PLS model based on first derivative values and selected wavelengths was less precise for assessing the Na content (Table 2), but the desired slope and offset are near 1.0 and 0.0, respectively (Figure 8).

Based on our results, an RPD value of 5.5 for Cl indicates that the calibration gave good results, whereas a value of 2.6 for Na indicates minimally acceptable performance.

Figures 9 and 10 present the measured *versus* predicted values applied to the external test set data using the models shown in Figures 7 and 8. For plant Cl content, applying our model to the external test set gave favourable prediction values, with RMSEP of 0.23,

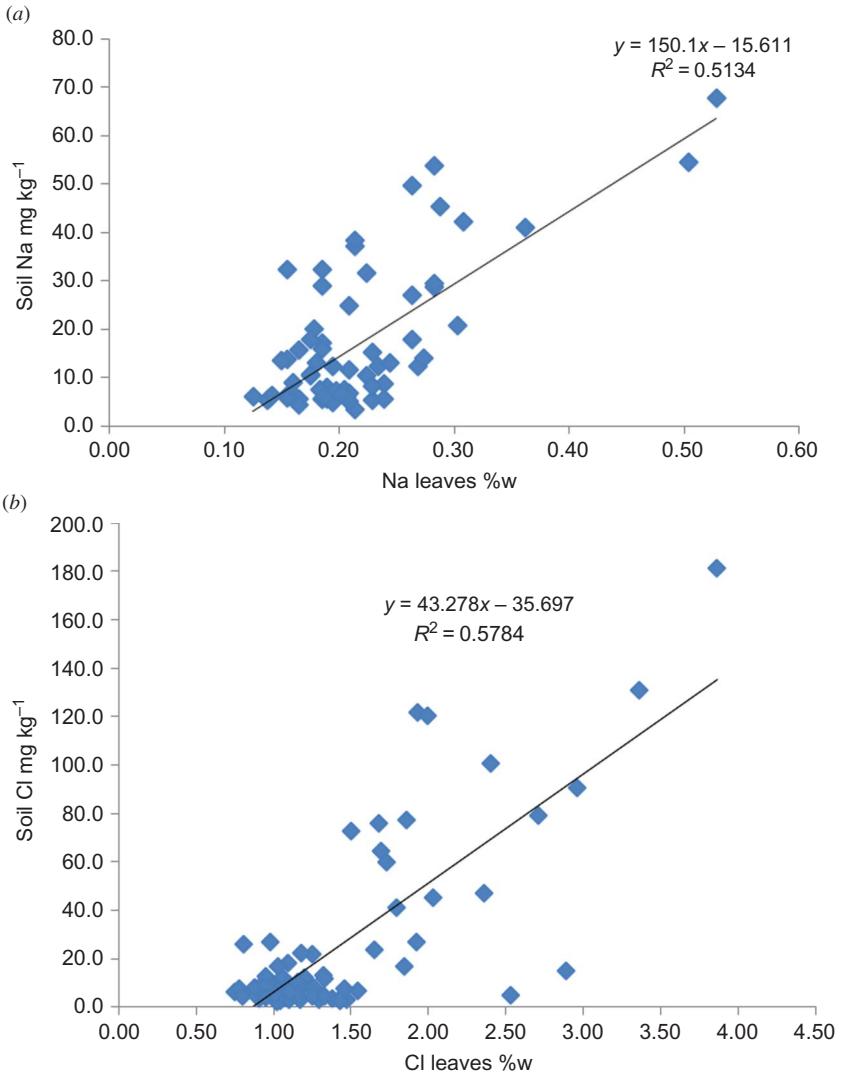

Figure 4. (*a*) Scatter plot of soil *versus* leaf Na content. (*b*) Scatter plot of soil *versus* leaf Cl content. Note: w, weight.

confirming the model's confidence level with five PLS components (Figure 9). For plant Na content, applying our model to an external test set of 15 samples provided an accuracy of 0.04, R^2 of 0.78, and RPD of 1.9 (Figure 10).

PLS models (first derivative) run on the whole wavelength region were found to be more complex (with 9–11 LV components) than models run on the individual wavelengths (3–5 LV components). The more complex models resulted in higher RMSEP and lower R^2 (for Cl content, RMSEP = 0.73 and R^2 = 0.62, whereas for Na content, RMSEP = 0.11 and R^2 = 0.4). Therefore, selection of specific wavelengths with reasonable spectral assignments is important to optimize spectroscopic modelling results. Furthermore, consideration of the spectra in different spectral units, run either on the whole wavelength region or on selected wavelengths, did not improve the accuracy of the final constructed models.

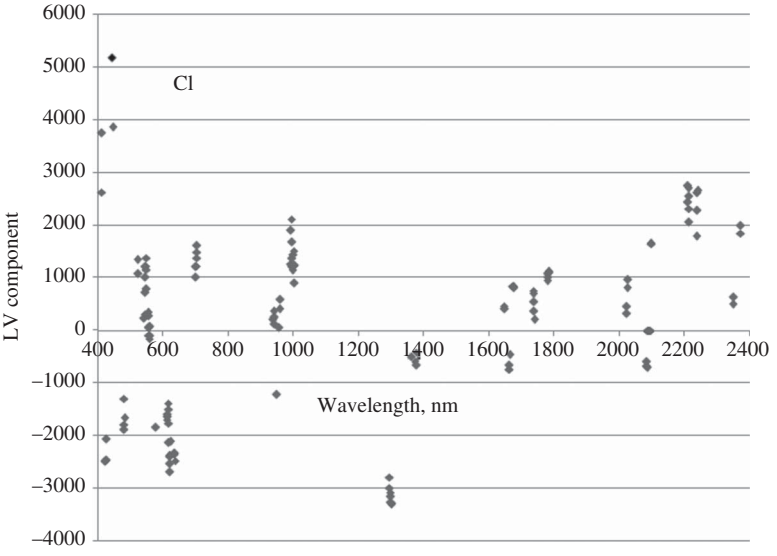

Figure 5. Partial least squares loading vectors (LV1-4) *versus* wavelength for the optimal calibration model for Cl content.

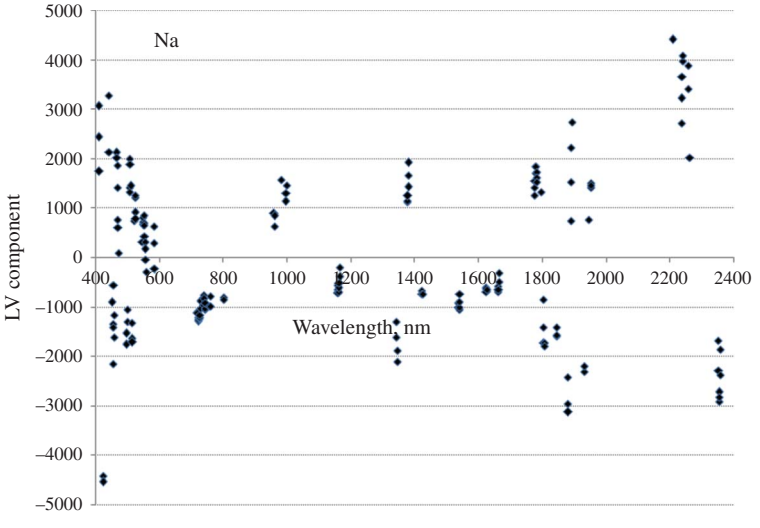

Figure 6. Partial least squares loading vectors (LV1-4) *versus* wavelength for the optimal calibration model for Na content.

In practice, more samples would be needed spanning a wide range of values (e.g. a chemical reference) to produce a more robust model. Nevertheless, these results suggest that soil reflectance spectroscopy is potentially useful for predicting soil and plant salinity. In addition, since there is a relatively small dynamic range of salt content measured in tomato leaves, even extremely small differences between the PLS model and reference values can increase RMSEP values. Furthermore, several samples were measured as having the same Cl or Na content, but spectrally predicted as having different contents, presumably due to lack of precision in either the reference measurement or calibration.

Table 2. Root mean square error of calibration (RMSEC) and coefficient of multiple determination (R^2) obtained for the calibration and cross-validation data sets for various data preprocessing techniques.

	Calibration		Prediction (external test set)		
	RMSECV		RMSEP		
Model	(%)	r^2	(%)	R^2	RPD
To assess Cl:					
Raw spectra	1.5	0.53	1.7	0.3	1.71
Spectra in Kubelka–Munk units	1.5	0.58	1.6	0.32	1.68
Absorbance	1.3	0.56	1.6	0.35	1.7
First derivative (whole spectral range)	0.73	0.62	0.8	0.46	2.5
First derivative (selected wavelengths)	0.2	0.92	0.23	0.93	5.5
Kubelka–Munk first derivative (selected wavelengths)	0.22	0.90	0.17	0.88	5.3
To assess Na:					
Raw spectra	0.15	0.36	0.17	0.55	1.60
Spectra in Kubelka–Munk units	0.18	0.35	0.18	0.52	1.52
Absorbance	0.18	0.31	0.18	0.52	1.6
First derivative (whole spectral range)	0.11	0.40	0.35	0.56	1.75
First derivative (selected wavelengths)	0.03	0.87	0.04	0.78	1.9
Kubelka–Munk first derivative (selected wavelengths)	0.04	0.85	0.08	0.74	1.9

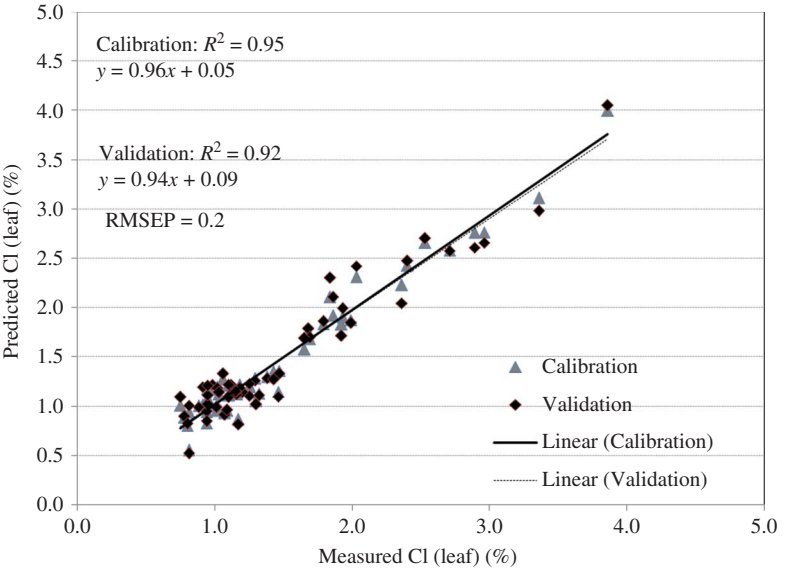

Figure 7. Scatter plot of measured *versus* predicted leaf Cl content for calibration and validation data sets.

4. Discussion and conclusions

The soils of the areas tested are saline mostly because they are influenced by a shallow saline water table. As halite (NaCl), which is the main salt product, does not have any spectral features in the VNIR region, it is difficult to use reflectance spectroscopy for its

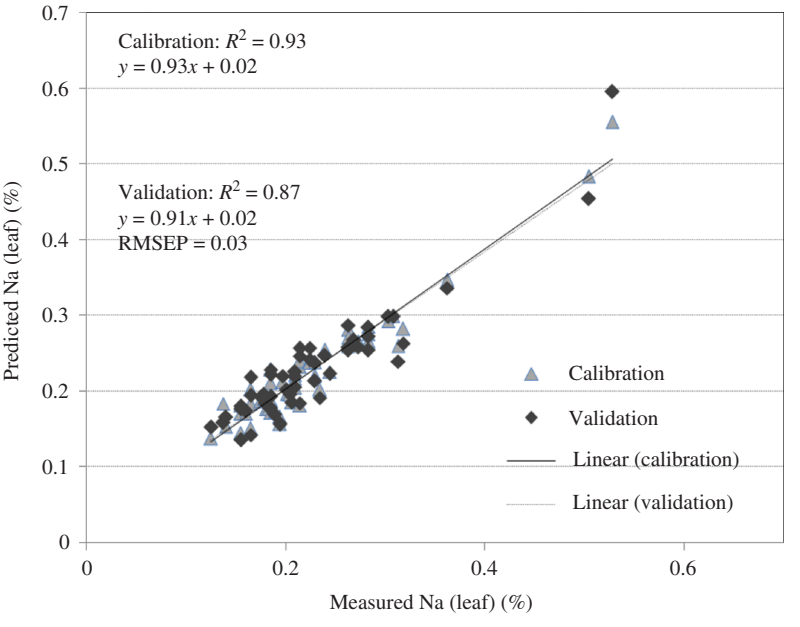

Figure 8. Scatter plot of measured *versus* predicted leaf Na content for calibration and validation data sets.

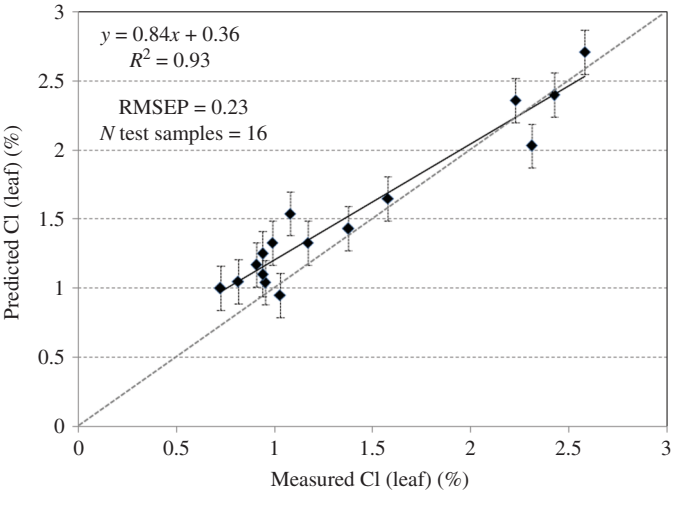

Figure 9. Scatter plot of measured *versus* predicted leaf Cl content for the cross-validation PLS model.

identification. However, Ben-Dor et al. (2009) found good correlation between soil-surface gypsum ($CaSO_4$) and halite concentration in soil-solution extracts taken from selected fields in Israel. In this study, we asked whether reflectance spectra of soil can predict the salinity status of tomato. To this end, we assessed the relationship between the leaf Na and Cl contents of tomato plants growing in a saline environment and their corresponding soil spectra measured in the laboratory by fitting PLS regression analyses. Specifically,

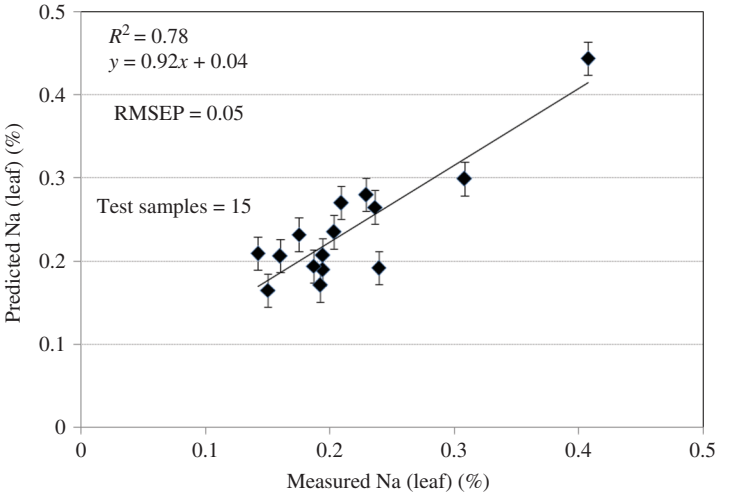

Figure 10. Scatter plot of measured *versus* predicted Na content for the cross-validation PLS model.

soil reflectance data were used to predict the Cl and Na contents in tomato plants. The PLS model aimed at predicting leaf Na content from soil reflectance spectra was less precise than the model aimed at predicting leaf Cl content. Importantly, in assessing tomato salinity by the presence of either plant Cl or Na content, the selection of specific wavelengths with reasonable spectral assignments is important and provides better results than using the entire wavelength spectrum.

Therefore, based on our results, we conclude that reflectance spectroscopy across the 400–2400 nm wavelength range can be used to assess plant salinity based on soil spectra. This conclusion supports timely decisions on crop water management. It should be noted that all samples were measured spectrally under laboratory conditions using a 'potato'. Further study is required to assess the relationships between soil salinity and crop Na or Cl status in a field setting. Furthermore, when *in situ* field measurements are collected in different environments with varying soil properties and salt contents, additional parameters might be considered such as soil moisture content, surface area of field of view (FOV), illumination type, and structure of the measured surface. Nevertheless, our results are sufficiently promising to suggest that future hyperspectral airborne remote-sensing measurements of soil salinity have a promising potential in the assessment of leaf salinity over farm fields. In this regard, the results of this study can serve as a starting point in precision agriculture for salinity measurements in tomato fields, and can be further upgraded to airborne/satellite remote-sensing modes. For instance, airborne remote sensing was used to assess the spatial distribution of soil salinity on a pixel-by-pixel basis (Goldshleger et al. 2012). This capability is especially important for distantly located and inaccessible areas, as it can provide information on environmental changes in soil and vegetation salinity changes.

Although salts lack spectral fingerprints across the NIR–SWIR spectral region, by using PLS regression analyses, we were able to assess quantitatively, with moderate accuracy, the salinity of tomato plants based on soil spectra. Although there was sufficient range in Na+ and Cl+ contents, the distribution of values was skewed to the minimum values. Future study is required to construct a more robust PLS model for implementation from field-to-field and area-to-area.

Another important issue that requires consideration in future research is the dependence of salt content on many different environmental factors such as climate conditions, topography, wind regime, and season, as well as anthropogenic activity (Metternicht and Zinck 2003). Therefore, the calibration models developed and used in this study (as shown in Figures 7 and 8) will not be geographically transferable because of the environmental differences among farm fields. In this regard, there is a need to examine the relationship between salt content and soil reflectance separately for different regions. PLS analysis of spectral measurements can be easily developed and applied to both.

Finally, this type of analysis can be further implemented to assess vegetation salinity ahead of planting, and could be developed as a generic tool for broader use worldwide. In this regard, for each field/study region, we suggest the assessment of threshold levels of salinity in tomato leaves and the taking of remedial action. An additional application is determination of tomato quality by monitoring long-term changes in soil salinity.

Acknowledgments

The authors greatly appreciate the comments by Dr Daniel Long, which significantly improved the current publication.

References

Ben-Dor, E., N. Goldshleger, M. Eshel, V. Mirablis, and U. Bason. 2009. "Combined Active and Passive Remote Sensing Methods for Assessing Soil Salinity." In *Remote Sensing of Soil Salinization: Impact and Land Management*, edited by G. Metternicht and A. Zinck, 235–255. Boca Raton, FL: CRC Press.

Clark, R. N. 1999. "Spectroscopy of Rocks and Minerals, and Principles of Spectroscopy." In *Manual of Remote Sensing,* edited by A. Rencz, 3–58. New York: John Wiley & Sons.

Cuartero, J., M. C. Bolari, M. J. Asi, and V. Moreno. 2006. "Increasing Salt Tolerance in the Tomato." *Journal of Experimental Botany* 57: 1045–1058.

Dan, Y., D. H. Yallon, H. Koyumdjisky, and Z. Raz. 1976. *The Soils of Israel*. Bet Dagan: The Volcani Institute of Agriculture, Pamphlet No. 159.

Demattê, J. A. M., R. C. Campos, M. C. Alves, P. R. Florid, and M. R. Nanni. 2004. "Visible–NIR Reflectance: A New Approach on Soil Evaluation." *Geoderma* 121: 95–111.

Esbensen, K. 2002. *Multivariate Data Analyses. An Introduction to Multivariate Data Analyses and Experimental Design*. 5th ed. Esbjerg: Aalborg University, CAMO Process AS. ISBN 82-99333032.

Gleick, P. H. 1993. "Water Resources: A Long-Range Global Evaluation." *Ecology Law Quarterly* 20: 141–149.

Goldshleger, I. Nlivne, A. A. Chudnovsky, and E. Ben-Dor. 2012. "Integrating Passive and Active Remote Sensing Methods to Assess Soil Salinity: A Case Study from Jezre'el Valley, Israel." *Applied and Environmental Soil Science* 177: 392–401.

Goldshleger, N., E. Ben-Dor, Y. Benyamini, and M. Agassi. 2004. "Soil Reflectance as a Tool for Assessing Physical Crust Arrangement of Four Typical Soils in Israel." *Soil Science* 169: 677–687.

Hille, D. 1998. *Envrironmental Soil Physics*. New York: Academic Press.

Hunt, G., J. Salisbury, and C. Lenhoff. 1972. "Visible and Near Infrared Spectra of Minerals and Rocks: V. Halides, Phosphates, Arsenates, Vanadates and Borates." *Modern Geology* 3: 121–132.

Hunt, G. R. 1977. "Spectral Signatures of Particulate Minerals, in the Visible and Near-Infrared." *Geophysics* 42: 501–513.

Kalra, Y. P. 1998. *Handbook of Reference Methods for Plant Analysis*. Soil and Plant Analysis Council. Boca Raton, FL: CRC Press.

Mark, H. (2000). "Quantitative Spectroscopic Calibration." In *Encyclopedia of Analytical Chemistry: Applications, Theory, and Instrumentation,* edited by R. A. Meyers. 15 vols. Chichester: John Wiley & Sons.

Metternicht, G. I. 1998. "Analyzing the Relationship between Ground Based Reflectance and Environment Indicators of Salinity Processes in the Cohabamba Valley (Bolivia)." *International Journal of Economic Environmental Science* 24: 359–370.

Metternicht, G. I., and J. A. Zinck. 2003. "Remote Sensing of Soil Salinity: Potentials and Constraints." *Remote Sensing of Environment* 85: 1–20.

Mirlas, V., Y. Benyamini, S. Marish, M. Gotesman, E. Fizik, and M. Agassi. 2003. "Method for Normalization of Soil Salinity Data." *Journal of the Irrigation and Drain Division, American Society of Civil Engineers* 129: 64–66.

Mouazen, A., M. Karouir, J. De Baerdemaeker, and H. Ramon. 2005. "Characterization of Soil Water Content Using Measured Visible and Near Infrared Spectra." *Soil Science Society of America Journal* 70: 1295–1302.

Mulders, M. A. 1987. *Remote Sensing in Soil Science, Developments in Soil Science*. Amsterdam: Elsevier.

Richards, L. A. 1954. *Diagnosis and Improvements of Saline and Alkali Soils*, 160p. Washington, DC: U.S. Salinity Laboratory DA, US Department of Agriculture Hbk 60.

Rud, R., M. Shoshany, and V. Alchanatis. 2011. "Spectral Indicators for Salinity Effects in Crops: A Comparison of a New Green Indigo Ratio with Existing Indices." *Remote Sensing Letters* 2: 289–298.

Savitzky, A., and M. J. E. Golay. 1964. "Smoothing and Differentiation of Data by Simplified Least Squares Procedures." *Analytical Chemistry* 36: 1627–1639.

Szabo, J., L. Pásztor, Z. Suba, and G. Varallyay. 1998. "Integration of Remote Sensing and GIS Techniques in Land Degradation Mapping. Pro-vegetation Indices in Crop Assessments." *Remote Sensing of Environment* 35: 105–119.

Wiegand, C., G. Anderson, S. Lingle, and D. Escobar. 1994. "Soil Salinity Effects on Crop Growth and Yield. Illustration of an Analysis and Mapping Methodology for Sugarcane." *Journal of Plant Physiology* 148: 418–424.

Williams, P., and K. Norris, eds. 1987. *Near-Infrared Technology in the Agricultural and Food Industriesi*. St. Paul, MN: American Association of Cereal Chemists.

Zhang, M., S. Ustin, E. Rejmankova, and E. Sanderson. 1997. "Monitoring Pacific Coast Salt Marshes Using Remote Sensing." *Ecological Applications* 7: 1039–1053.

Zinck, U., and G. Metternicht. 2009. "Soil Salinity and Salinization Hazard." In *Remote Sensing of Soil Salinization: Impact and Land Management*, edited by G. Metternicht and A. Zinck, 3–20. Boca Raton, FL: CRC Press.